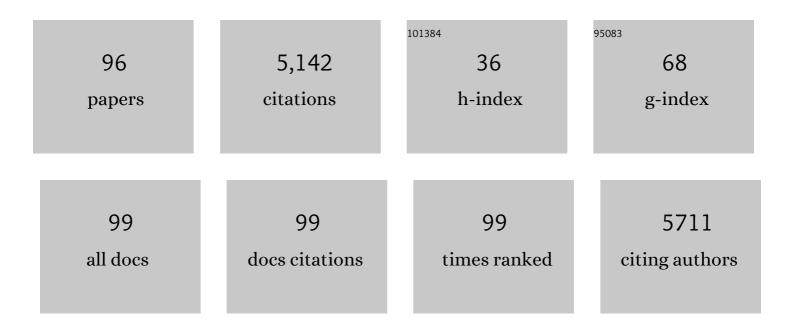
Qianling Zhang

List of Publications by Year in descending order

Source: https://exaly.com/author-pdf/929499/publications.pdf Version: 2024-02-01



#	Article	IF	CITATIONS
1	A universal, facile and ultrafast monomer-tuned strategy to construct multi-dimensional hierarchical polymer structures and applications for lithium-ion batteries. Chemical Engineering Journal, 2022, 428, 131135.	6.6	10
2	Sonodynamic cancer therapy by novel iridium-gold nanoassemblies. Chinese Chemical Letters, 2022, 33, 1907-1912.	4.8	16
3	Efficient capture and conversion of polysulfides by zinc protoporphyrin framework-embedded triple-layer nanofiber separator for advanced Li-S batteries. Journal of Colloid and Interface Science, 2022, 609, 43-53.	5.0	9
4	Deeply self-reconstructing CoFe(H3O)(PO4)2 to low-crystalline Fe0.5Co0.5OOH with Fe3+–O–Fe3+ motifs for oxygen evolution reaction. Applied Catalysis B: Environmental, 2022, 304, 120986.	10.8	36
5	Elucidating the activity, mechanism and application of selective electrosynthesis of ammonia from nitrate on cobalt phosphide. Energy and Environmental Science, 2022, 15, 760-770.	15.6	133
6	N-Doped Graphene Supported Cu Single Atoms: Highly Efficient Recyclable Catalyst for Enhanced C–N Coupling Reactions. ACS Nano, 2022, 16, 1142-1149.	7.3	36
7	Rational design of Ru species on N-doped graphene promoting water dissociation for boosting hydrogen evolution reaction. Science China Chemistry, 2022, 65, 521-531.	4.2	12
8	An ultrasound activated cyanine-rhenium(<scp>i</scp>) complex for sonodynamic and gas synergistic therapy. Chemical Communications, 2022, 58, 3314-3317.	2.2	22
9	Band Engineering Induced Conducting 2Hâ€Phase MoS ₂ by PdSRe Sites Modification for Hydrogen Evolution Reaction. Advanced Energy Materials, 2022, 12, .	10.2	37
10	Ruthenium photosensitizer anchored gold nanorods for synergistic photodynamic and photothermal therapy. Dalton Transactions, 2022, 51, 6846-6854.	1.6	5
11	A cerium-doped NASICON chemically coupled poly(vinylidene fluoride-hexafluoropropylene)-based polymer electrolyte for high-rate and high-voltage quasi-solid-state lithium metal batteries. Journal of Energy Chemistry, 2022, 73, 311-321.	7.1	11
12	Fluorine-free prepared two-dimensional molybdenum boride (MBene) as a promising anode for lithium-ion batteries with superior electrochemical performance. Chemical Engineering Journal, 2022, 446, 137466.	6.6	27
13	Ultrathin MoS2 anchored on 3D carbon skeleton containing SnS quantum dots as a high-performance anode for advanced lithium ion batteries. Chemical Engineering Journal, 2021, 403, 126251.	6.6	105
14	Amorphous MoS3 decoration on 2D functionalized MXene as a bifunctional electrode for stable and robust lithium storage. Chemical Engineering Journal, 2021, 406, 126775.	6.6	59
15	Sulfurâ€Coordinated Organoiridium(III) Complexes Exert Breast Anticancer Activity via Inhibition of Wnt/β atenin Signaling. Angewandte Chemie - International Edition, 2021, 60, 4841-4848.	7.2	16
16	Engineering defect-rich Fe-doped NiO coupled Ni cluster nanotube arrays with excellent oxygen evolution activity. Applied Catalysis B: Environmental, 2021, 285, 119809.	10.8	103
17	Construction of cobalt oxyhydroxide nanosheets with rich oxygen vacancies as high-performance lithium-ion battery anodes. Journal of Materials Chemistry A, 2021, 9, 453-462.	5.2	47
18	Co–Mo–P carbon nanospheres derived from metal–organic frameworks as a high-performance electrocatalyst towards efficient water splitting. Journal of Materials Chemistry A, 2021, 9, 1143-1149.	5.2	36

#	Article	IF	CITATIONS
19	Recent development and application of cyclometalated iridium(<scp>iii</scp>) complexes as chemical and biological probes. Dalton Transactions, 2021, 50, 6410-6417.	1.6	37
20	<i>In situ</i> formed lithium ionic conductor thin film on the surface of high-crystal-layered LiCoO ₂ as a high-voltage cathode material. Materials Chemistry Frontiers, 2021, 5, 6171-6181.	3.2	8
21	Carbon nanotubes coupled with layered graphite to support SnTe nanodots as high-rate and ultra-stable lithium-ion battery anodes. Nanoscale, 2021, 13, 3782-3789.	2.8	23
22	Synthesis of V-notched half-open polymer microspheres <i>via</i> facile solvent-tuned self-assembly. New Journal of Chemistry, 2021, 45, 13964-13968.	1.4	1
23	Molecular design of stapled pentapeptides as building blocks of self-assembled coiled coil–like fibers. Science Advances, 2021, 7, .	4.7	12
24	Electrochemical Construction of Low-Crystalline CoOOH Nanosheets with Short-Range Ordered Grains to Improve Oxygen Evolution Activity. ACS Catalysis, 2021, 11, 6104-6112.	5.5	103
25	Water-Soluble Iridic–Porphyrin Complex for Non-invasive Sonodynamic and Sono-oxidation Therapy of Deep Tumors. ACS Applied Materials & Interfaces, 2021, 13, 27934-27944.	4.0	39
26	Ruthenium Complexes as Promising Candidates against Lung Cancer. Molecules, 2021, 26, 4389.	1.7	32
27	Diatom-like silica–protein nanocomposites for sustained drug delivery of ruthenium polypyridyl complexes. Journal of Inorganic Biochemistry, 2021, 221, 111489.	1.5	9
28	A highly potent ruthenium(II)-sonosensitizer and sonocatalyst for in vivo sonotherapy. Nature Communications, 2021, 12, 5001.	5.8	78
29	Ultra″ow″oaded Niâ^'Fe Dimer Anchored to Nitrogen/Oxygen Sites for Boosting Electroreduction of Carbon Dioxide. ChemSusChem, 2021, 14, 4499-4506.	3.6	9
30	A blended gel polymer electrolyte for dendrite-free lithium metal batteries. Applied Surface Science, 2021, 569, 150899.	3.1	18
31	Multiple anionic Ni(SO4)0.3(OH)1.4 nanobelts/reduced graphene oxide enabled by enhanced multielectron reactions with superior lithium storage capacity. Chemical Engineering Journal, 2021, 426, 131863.	6.6	3
32	Tuning and understanding the electronic effect of Co–Mo–O sites in bifunctional electrocatalysts for ultralong-lasting rechargeable zinc–air batteries. Journal of Materials Chemistry A, 2021, 9, 21716-21722.	5.2	16
33	ZIF-derived "senbei―like Co ₉ S ₈ /CeO ₂ /Co heterostructural nitrogen-doped carbon nanosheets as bifunctional oxygen electrocatalysts for Zn-air batteries. Nanoscale, 2021, 13, 3227-3236.	2.8	33
34	Bifunctional oxygen electrocatalysis on ultra-thin Co ₉ S ₈ /MnS carbon nanosheets for all-solid-state zinc–air batteries. Journal of Materials Chemistry A, 2021, 9, 22635-22642.	5.2	22
35	Rapid ionic conductivity of ternary composite electrolytes for superior solid-state batteries with high-rate performance and long cycle life operated at room temperature. Journal of Materials Chemistry A, 2021, 9, 18338-18348.	5.2	23
36	Metal complexes against breast cancer stem cells. Dalton Transactions, 2021, 50, 14498-14512.	1.6	36

#	Article	IF	CITATIONS
37	Unveiling the reaction mechanism of an Sb ₂ S ₃ –Co ₉ 8/NC anode for high-performance lithium-ion batteries. Nanoscale, 2021, 13, 20041-20051.	2.8	13
38	Nonmetal Doping as a Robust Route for Boosting the Hydrogen Evolution of Metalâ€Based Electrocatalysts. Chemistry - A European Journal, 2020, 26, 3930-3942.	1.7	15
39	Highly efficient utilization of single atoms via constructing 3D and free-standing electrodes for CO2 reduction with ultrahigh current density. Nano Energy, 2020, 70, 104454.	8.2	106
40	NAMI-A preferentially reacts with the Sp1 protein: understanding the anti-metastasis effect of the drug. Chemical Communications, 2020, 56, 1397-1400.	2.2	13
41	A HCBP1 peptide conjugated ruthenium complex for targeted therapy of hepatoma. Dalton Transactions, 2020, 49, 972-976.	1.6	4
42	Unconventionally fabricating defect-rich NiO nanoparticles within ultrathin metal–organic framework nanosheets to enable high-output oxygen evolution. Journal of Materials Chemistry A, 2020, 8, 2140-2146.	5.2	66
43	Boosting the alkaline hydrogen evolution of Ru nanoclusters anchored on B/N–doped graphene by accelerating water dissociation. Nano Energy, 2020, 68, 104301.	8.2	138
44	One-pot synthesis of N,S-doped pearl chain tube-loaded Ni3S2 composite materials for high-performance lithium–air batteries. Nanoscale, 2020, 12, 21770-21779.	2.8	7
45	A unique space confined strategy to construct defective metal oxides within porous nanofibers for electrocatalysis. Energy and Environmental Science, 2020, 13, 5097-5103.	15.6	80
46	Near-infrared phosphorescent terpyridine osmium(<scp>ii</scp>) photosensitizer complexes for photodynamic and photooxidation therapy. Inorganic Chemistry Frontiers, 2020, 7, 4020-4027.	3.0	13
47	Removing the barrier to water dissociation on single-atom Pt sites decorated with a CoP mesoporous nanosheet array to achieve improved hydrogen evolution. Journal of Materials Chemistry A, 2020, 8, 11246-11254.	5.2	62
48	Highâ€Performance Overall CO ₂ Splitting on Hierarchical Structured Cobalt Disulfide with Partially Removed Sulfur Edges. Advanced Functional Materials, 2020, 30, 2000154.	7.8	26
49	Slower Removing Ligands of Metal Organic Frameworks Enables Higher Electrocatalytic Performance of Derived Nanomaterials. Small, 2020, 16, e2002210.	5.2	47
50	Microenvironment-sensitive iridium(<scp>iii</scp>) complexes for disease theranostics. Dalton Transactions, 2020, 49, 9182-9190.	1.6	9
51	Two dimensional ZIF-derived ultra-thin Cu–N/C nanosheets as high performance oxygen reduction electrocatalysts for high-performance Zn–air batteries. Nanoscale, 2020, 12, 14259-14266.	2.8	34
52	In situ encapsulated and well dispersed Co3O4 nanoparticles as efficient and stable electrocatalysts for high-performance CO2 reduction. Journal of Materials Chemistry A, 2020, 8, 15675-15680.	5.2	24
53	Recent Progress in Self‣upported Catalysts for CO ₂ Electrochemical Reduction. Small Methods, 2020, 4, 1900826.	4.6	48
54	Carbon dioxide electroreduction on single-atom nickel decorated carbon membranes with industry compatible current densities. Nature Communications, 2020, 11, 593.	5.8	330

#	Article	IF	CITATIONS
55	Construction of tetrahedral CoO ₄ vacancies for activating the high oxygen evolution activity of Co _{3â^'x} O _{4â^'δ} porous nanosheet arrays. Nanoscale, 2020, 12, 11079-11087.	2.8	35
56	Frontispiece: Nonmetal Doping as a Robust Route for Boosting the Hydrogen Evolution of Metalâ€Based Electrocatalysts. Chemistry - A European Journal, 2020, 26, .	1.7	0
57	Recent advances in lysosome-targeting luminescent transition metal complexes. Coordination Chemistry Reviews, 2019, 398, 113010.	9.5	45
58	Approaching Durable Single-Layer Fuel Cells: Promotion of Electroactivity and Charge Separation via Nanoalloy Redox Exsolution. ACS Applied Materials & Interfaces, 2019, 11, 27924-27933.	4.0	74
59	Unconventional molybdenum carbide phases with high electrocatalytic activity for hydrogen evolution reaction. Journal of Materials Chemistry A, 2019, 7, 18030-18038.	5.2	64
60	Electronic structure engineering of single atomic Ru by Ru nanoparticles to enable enhanced activity for alkaline water reduction. Journal of Materials Chemistry A, 2019, 7, 19531-19538.	5.2	33
61	Nanomeshes: General Synthesis of Ultrathin Metal Borate Nanomeshes Enabled by 3D Barkâ€Like Nâ€Doped Carbon for Electrocatalysis (Adv. Energy Mater. 28/2019). Advanced Energy Materials, 2019, 9, 1970109.	10.2	3
62	Scalable Production of Efficient Single-Atom Copper Decorated Carbon Membranes for CO ₂ Electroreduction to Methanol. Journal of the American Chemical Society, 2019, 141, 12717-12723.	6.6	545
63	Interconnected phosphorus-doped CoO-nanoparticles nanotube with three-dimensional accessible surface enables high-performance electrochemical oxidation. Nano Energy, 2019, 66, 104194.	8.2	35
64	The stepwise photodamage of organelles by two-photon luminescent ruthenium(<scp>ii</scp>) photosensitizers. Chemical Communications, 2019, 55, 11235-11238.	2.2	24
65	Au@Prussian Blue Hybrid Nanomaterial Synergy with a Chemotherapeutic Drug for Tumor Diagnosis and Chemodynamic Therapy. ACS Applied Materials & amp; Interfaces, 2019, 11, 39493-39502.	4.0	47
66	Highly stable single Pt atomic sites anchored on aniline-stacked graphene for hydrogen evolution reaction. Energy and Environmental Science, 2019, 12, 1000-1007.	15.6	392
67	Coupling pentlandite nanoparticles and dual-doped carbon networks to yield efficient and stable electrocatalysts for acid water oxidation. Journal of Materials Chemistry A, 2019, 7, 461-468.	5.2	54
68	Superhydrophilic Phyticâ€Acidâ€Doped Conductive Hydrogels as Metalâ€Free and Binderâ€Free Electrocatalysts for Efficient Water Oxidation. Angewandte Chemie - International Edition, 2019, 58, 4318-4322.	7.2	168
69	Recent progress in the hybrids of transition metals/carbon for electrochemical water splitting. Journal of Materials Chemistry A, 2019, 7, 14380-14390.	5.2	111
70	General Synthesis of Ultrathin Metal Borate Nanomeshes Enabled by 3D Bark‣ike Nâ€Đoped Carbon for Electrocatalysis. Advanced Energy Materials, 2019, 9, 1901130.	10.2	46
71	A phosphorescent iridium probe for sensing polarity in the endoplasmic reticulum and <i>in vivo</i> . Dalton Transactions, 2019, 48, 7728-7734.	1.6	11
72	A viscosity-sensitive iridium(<scp>iii</scp>) probe for lysosomal microviscosity quantification and blood viscosity detection in diabetic mice. Dalton Transactions, 2019, 48, 3990-3997.	1.6	25

#	Article	IF	CITATIONS
73	Zn–Air Batteries: Trifunctional Electrocatalysis on Dualâ€Đoped Graphene Nanorings–Integrated Boxes for Efficient Water Splitting and Zn–Air Batteries (Adv. Energy Mater. 14/2019). Advanced Energy Materials, 2019, 9, 1970045.	10.2	3
74	Facile synthesis of polyacrylonitrile-based N/S-codoped porous carbon as an efficient oxygen reduction electrocatalyst for zinc–air batteries. Journal of Materials Chemistry A, 2019, 7, 11223-11233.	5.2	39
75	Superhydrophilic Phyticâ€Acidâ€Doped Conductive Hydrogels as Metalâ€Free and Binderâ€Free Electrocatalysts for Efficient Water Oxidation. Angewandte Chemie, 2019, 131, 4362-4366.	1.6	29
76	Design of ruthenium-albumin hydrogel for cancer therapeutics and luminescent imaging. Journal of Inorganic Biochemistry, 2019, 194, 19-25.	1.5	22
77	Trifunctional Electrocatalysis on Dualâ€Doped Graphene Nanorings–Integrated Boxes for Efficient Water Splitting and Zn–Air Batteries. Advanced Energy Materials, 2019, 9, 1803867.	10.2	173
78	lsomeric lr(<scp>iii</scp>) complexes for tracking mitochondrial pH fluctuations and inducing mitochondrial dysfunction during photodynamic therapy. Dalton Transactions, 2019, 48, 17200-17209.	1.6	16
79	Charge-Selective Delivery of Proteins Using Mesoporous Silica Nanoparticles Fused with Lipid Bilayers. ACS Applied Materials & Interfaces, 2019, 11, 3645-3653.	4.0	30
80	A novel iridium(<scp>iii</scp>) complex for sensitive HSA phosphorescence staining in proteome research. Chemical Communications, 2018, 54, 3282-3285.	2.2	14
81	Chirality in metal-based anticancer agents. Dalton Transactions, 2018, 47, 4017-4026.	1.6	43
82	Facile fabrication of a 3D network composed of N-doped carbon-coated core–shell metal oxides/phosphides for highly efficient water splitting. Sustainable Energy and Fuels, 2018, 2, 1085-1092.	2.5	40
83	"Turn off-on―phosphorescent sensor for biothiols based on a Ru-Cu ensemble. Sensors and Actuators B: Chemical, 2018, 255, 283-289.	4.0	22
84	Composition Tailoring via N and S Coâ€doping and Structure Tuning by Constructing Hierarchical Pores: Metalâ€Free Catalysts for Highâ€Performance Electrochemical Reduction of CO ₂ . Angewandte Chemie, 2018, 130, 15702-15706.	1.6	63
85	Composition Tailoring via N and S Coâ€doping and Structure Tuning by Constructing Hierarchical Pores: Metalâ€Free Catalysts for Highâ€Performance Electrochemical Reduction of CO ₂ . Angewandte Chemie - International Edition, 2018, 57, 15476-15480.	7.2	162
86	Near-Infrared Luminescent Osmium(II) Complexes with an Intrinsic RNA-Targeting Capability for Nucleolus Imaging in Living Cells. ACS Applied Bio Materials, 2018, 1, 1587-1593.	2.3	18
87	Carbothermal Synthesis of Nitrogen-Doped Graphene Composites for Energy Conversion and Storage Devices. Frontiers in Chemistry, 2018, 6, 501.	1.8	11
88	Boosting Electrochemical Hydrogen Evolution of Porous Metal Phosphides Nanosheets by Coating Defective TiO ₂ Overlayers. Small, 2018, 14, e1802755.	5.2	45
89	Crafting MoC2-doped bimetallic alloy nanoparticles encapsulated within N-doped graphene as roust bifunctional electrocatalysts for overall water splitting. Nano Energy, 2018, 50, 212-219.	8.2	205
90	Redox route to ultrathin metal sulfides nanosheet arrays-anchored MnO 2 nanoparticles as self-supported electrocatalysts for efficient water splitting. Journal of Power Sources, 2018, 398, 159-166.	4.0	43

#	Article	IF	CITATIONS
91	Tuning peptide self-assembly by an in-tether chiral center. Science Advances, 2018, 4, eaar5907.	4.7	50
92	Tracking mitochondrial dynamics during apoptosis with phosphorescent fluorinated iridium(iii) complexes. Dalton Transactions, 2018, 47, 12907-12913.	1.6	9
93	In–situ Characterization and Cure Kinetics in NEPE Propellant/ HTPB Liner Interface by Microscopic FTâ€IR. Propellants, Explosives, Pyrotechnics, 2017, 42, 410-416.	1.0	12
94	A NIR phosphorescent osmium(<scp>ii</scp>) complex as a lysosome tracking reagent and photodynamic therapeutic agent. Chemical Communications, 2017, 53, 12341-12344.	2.2	52
95	Development of a high quantum yield dye for tumour imaging. Chemical Science, 2017, 8, 6322-6326.	3.7	51
96	Polypyridyl Complexes of Ruthenium(II): Stabilization of Gâ€quadruplex DNA and Inhibition of Telomerase Activity. ChemPlusChem, 2012, 77, 551-562.	1.3	18